ACS central science

http://pubs.acs.org/journal/acscii

Research Article

Optically Manipulated Neutrophils as Native Microcrafts *In Vivo*

Xiaoshuai Liu,[#] Qing Gao,[#] Shuai Wu, Haifeng Qin, Tiange Zhang, Xianchuang Zheng,[*] and Baojun Li[*]

Cite This: *ACS Cent. Sci.* 2022, 8, 1017−1027

Read Online

ACCESS | Metrics & More | Article Recommendations | Supporting Information

ABSTRACT: As the first line of host defense against invading pathogens, neutrophils have an inherent phagocytosis capability for the elimination of foreign agents and target loading upon activation, as well as the ability to transmigrate across blood vessels to the infected tissue, making them natural candidates to execute various medical tasks *in vivo*. However, most of the existing neutrophil-based strategies rely on their spontaneous chemotactic motion, lacking in effective activation, rapid migration, and high navigation precision. Here, we report an optically manipulated neutrophil microcraft *in vivo* through the organic integration of endogenous neutrophils and scanning optical tweezers, functioning as a native biological material and wireless remote controller, respectively. The neutrophil microcrafts can be remotely activated by light and then navigated to the target position along a designated route, followed by the fulfillment of its task *in vivo*, such as active intercellular connection, targeted delivery of nanomedicine, and precise elimination of cell debris, free from the extra construction or modification of the native neutrophils. On the basis of the innate immunologic function of neutrophils and intelligent optical manipulation, the proposed neutrophil microcraft might provide new insight for the construction of native medical microdevices for drug delivery and precise treatment of inflammatory diseases.

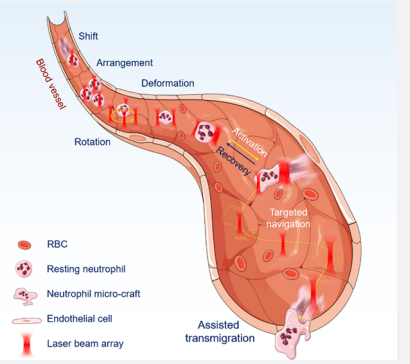

INTRODUCTION

By the organic integration of untethered microstructures and specific propulsion mechanisms *in vivo*, medical microdevices have attracted great attention in the biotechnology and precision medicine fields,[1−3] especially for active target delivery and pathogen clearance in the circulatory system.[4−6] With the assistance of intelligent locomotion control and efficient assignment execution, medical microdevices could achieve a precise therapeutic payload and then deliver them directly into target regions, with great potential to improve therapeutic efficacy while reducing possible side effects.[7−11] However, because of their foreign nature, an invasive implantation is usually required to introduce the synthetic matter into blood vessels and thus might disrupt the normal physiological environment.[12−14] Once entering the body, they tend to trigger the immune response and require an elaborate surface decoration to avoid immune clearance and extend the circulation time.[15] More importantly, they face great challenges to cross the natural biological barriers, i.e., the vessel walls, and thus are hard to penetrate into the tissue to accomplish complex medical tasks.[16]

With high biocompatibility and minor immunogenicity, endogenous blood cells have been proposed for constructing multifunctional medical microrobots, free from invasive implantation and tissue damage.[17−19] These strategies integrate biological materials with microrobotic principles in an organic manner, thus bridging the gap between the synthetic machine and biological world.[20] Among them, red blood cells (RBCs) have been proposed for constructing biocompatible micromotors or microrobots due to their abundance, prolonged circulation, high biocompatibility, and excellent surface immunosuppressive properties.[21,22] However, for potential pathogen clearance and drug delivery, they might face great challenges to achieve deep penetration across biological barriers and active navigation toward inflammation sites. On the other hand, as the first line of host defense against invading pathogens,[23,24] neutrophils have inherent phagocytosis capability for the elimination of foreign agents upon activation.[25] In addition, they can serve as carriers for target loading via phagocytosis[26,27] and have the ability to transmigrate across blood vessels to the infected tissue,[28−30] making them natural candidates for the construction of medical microdevices *in vivo*. However, most of the existing neutrophil-based strategies rely on the spontaneous chemotactic motion, lacking in effective activation, rapid migration, and high navigation precision.[31] Moreover, some stray neutrophils might enter the normal tissue rather than inflammation sites, thus inducing a series of undesired chronic inflammation events.[32] Therefore, an untethered technique needs to be introduced to manipulate the neutrophils' behavior *in vivo* so

Received: April 20, 2022
Published: July 13, 2022

https://doi.org/10.1021/acscentsci.2c00468
ACS Cent. Sci. 2022, 8, 1017−1027

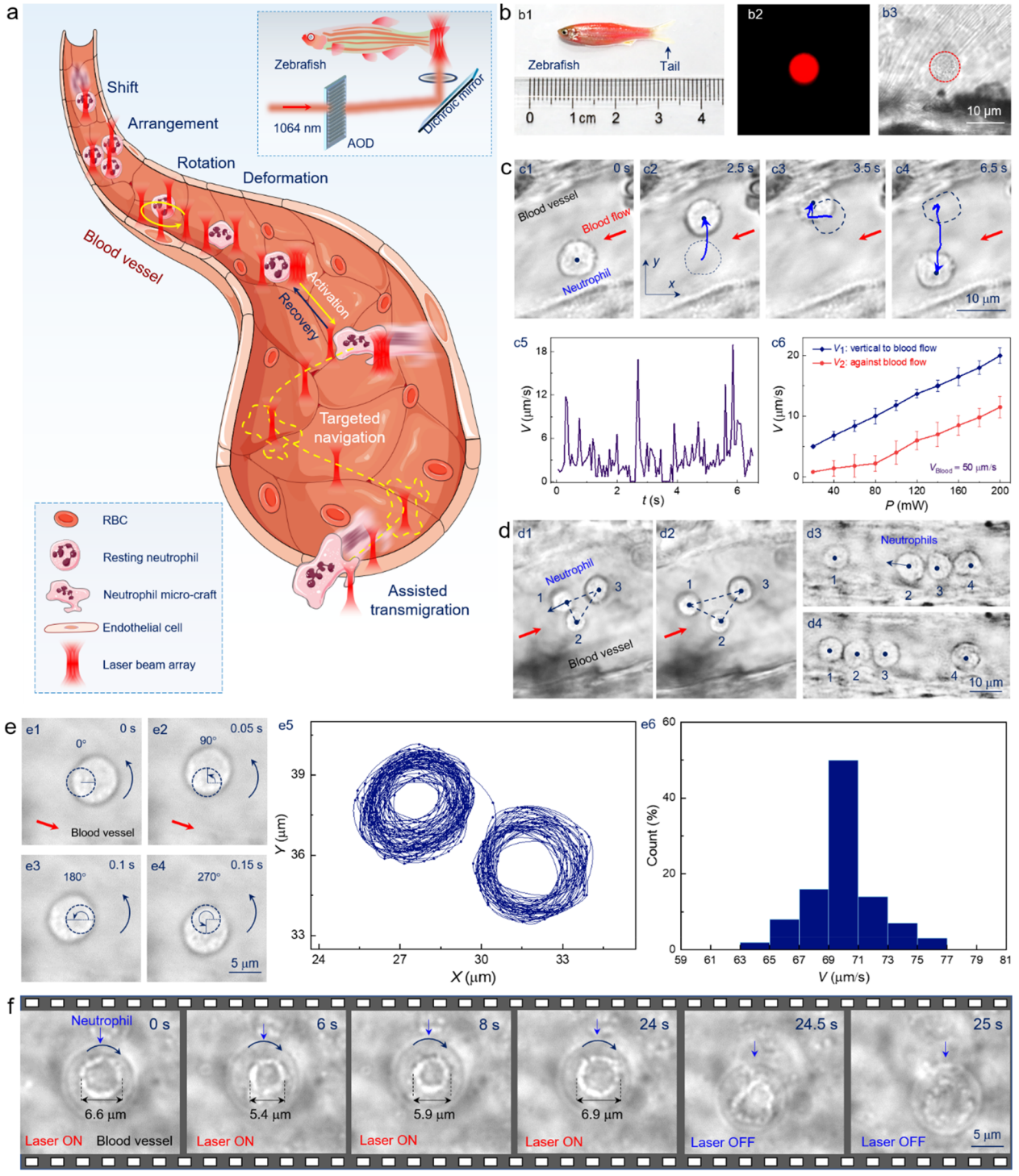

Figure 1. (a) Schematic illustration for optically manipulated neutrophil microcraft *in vivo*. (b) Optical microscopic images of zebrafish (b1) and fluorescence-labeled neutrophils (b2 and b3). (c) Dynamic manipulation of resting neutrophils (c1−c4) with a detailed velocity (c5) and acquired maximum motion velocity for shifting the neutrophil vertical to and against blood flow (c6). (d) Precise arrangement of multiple neutrophils into a triangle shape (d1 and d2) or in a line (d3 and d4). (e) Controlled revolution of one neutrophil in the blood vessel (e1−e4) with the tracked motion trajectory of the cell center (e5) and calculated velocity distribution (e6). (f) Optical microscopic images for rotating granules in the intravital neutrophil with an adjustable diameter.

that they can execute medical tasks in an actively controllable manner.

So far, various strategies have been developed to manipulate neutrophils, including atom force microscopy,[33] microfluidic techniques,[34] magnetic fields,[31] and optical tweezers.[35] Among them, optical tweezers have exhibited great potential for manipulating blood cells *in vivo*, due to their contactless and noninvasive nature, single-cell precision, and being free from strict limitations on the specific material property.[36] The feasibility of manipulating neutrophils with optical tweezers has been demonstrated *in vitro*,[35] but the optical manipulation of neutrophils *in vivo* for exploring potential biomedical

https://doi.org/10.1021/acscentsci.2c00468
ACS Cent. Sci. 2022, 8, 1017−1027

applications has not been reported. In this work, with the assistance of programmable optical manipulation, the precise control of biological activities of neutrophils has been performed *in vivo*, including remote activation, targeted navigation, and assisted transmigration, thus transforming the natural neutrophil into a native cellular microcraft. Furthermore, three potential applications were explored for the proposed neutrophil microcraft *in vivo*, including active cell connection, targeted delivery of nanomedicine, and elimination of cell debris. By integrating the noninvasive manipulation of optical tweezers and innate immunologic function of neutrophils, the proposed neutrophil microcraft provides new insight for the construction of native medical microdevices for precision medicine *in vivo*.

RESULTS AND DISCUSSION

Design of Optically Manipulated Neutrophil Microcraft and Experiment Setup. A schematic illustration of the optically manipulated neutrophil microcraft *in vivo* is shown in Figure 1a. With the assistance of scanning optical tweezers (SOTs), a flowing neutrophil can be stably trapped in the blood vessel by optical gradient force. After that, intelligent behavior control was conducted for the neutrophil in a programmable manner. The basic actions of the neutrophil can be fully manipulated, such as directional movement, precise arrangement, controlled rotation, and dynamic deformation. Furthermore, by stretching the neutrophil with two laser beams in a cyclic manner, the pseudopodium can be induced in a designated direction, thus switching the neutrophil to the activation state. By the precise regulation of SOTs, the activated neutrophil can be navigated to the targeted region along a designed route *in vivo*. Additionally, the optical force can guide and promote the transmigration of the activated neutrophil across biological barriers, such as the vessel wall. During the above processes, the optical force can be regarded as a wireless key for remote activation, a steering wheel for navigation, and an engine for actuation. Meanwhile, the neutrophil keeps its innate functions such as phagocytosis and drug loading for further applications. In this way, a native neutrophil microcraft can be constructed *in vivo* through the organic integration of endogenous neutrophils and programmable optical manipulation.

The experiment setup is shown in the inset of Figure 1a. The laser beam at a wavelength of 1064 nm was chosen because the biological tissue has a weak absorption for it, thus minimizing potential photothermal or photodynamic damages.[37] The laser beam was first interacted with an acoustic-optical deflector (AOD) to achieve a desired spatiotemporal distribution (maximum switching rate: 100 kHz). Then, the laser beam was reflected by a dichroic mirror and focused through a 60× water immersion microscope. Finally, the focused laser beam was irradiated on zebrafish to conduct multifunctional manipulation of neutrophils *in vivo*. The zebrafish was selected as the animal model in this study due to its high genome homology with humans[38] and readily observable blood circulation in the zebrafish tail for optical manipulation (Figure 1b1), in which the neutrophils were clearly identified through fluorescence labeling (Figures 1b2 and 3).

Motion Control of the Neutrophil Microcraft *In Vivo*. To demonstrate the operation flexibility of SOTs on the neutrophil microcraft, a series of motion controls were performed for the resting neutrophils *in vivo*, including directional movement, precise arrangement, and controlled rotation. As indicated in Figure 1c, a neutrophil flowed in the blood vessel with a velocity of 10 μm/s. At t = 0 s, an optical trap was exerted at the cell center (indicated by the navy dot), and the neutrophil stopped flowing at once. Then, the neutrophil was shifted along the $+y$ direction by the programmed movement of a laser beam controlled by AOD, with the motion trajectory indicated by the blue curve (Figure 1c2). Afterward, it was moved toward the $-x$ direction and followed by the $+y$ direction, to draw an "L"-shaped motion trajectory from 2.5 to 3.5 s (Figure 1c3). Finally, the neutrophil was moved back to its original location at t = 6.5 s along the $-y$ direction (Figure 1c4). During this process, the shift velocity ranged from 0 to 19 μm/s, with an average value of 5 μm/s (Figure 1c5). Furthermore, the operation flexibility was characterized by shifting the neutrophil along the direction vertical to the blood flow and against blood flow (V_{Blood} = 50 μm/s), as indicated by the blue and red curve in Figure 1c6, respectively. The acquired shift velocity increased with laser power due to the increased optical force, and meanwhile a larger velocity was obtained for the dynamical shift vertical to blood flow because of the smaller flow resistance.

In addition to the single neutrophil, multiple neutrophils could be manipulated simultaneously and arranged into various patterns. As indicated in Figure 1d1, three neutrophils were assembled into a rectangular triangle shape, which was further adjusted to the shape of equicrural triangle (Figure 1d2 and Movie S1). Besides the static patterning, a dynamic regulation was performed for multiple neutrophils. As indicated in Figures 1d3 and 4, four neutrophils flowing in the blood vessel were arranged into a line, and their relative positions could undergo a precise regulation by the SOTs. The number of manipulated neutrophils could be further increased; e.g., five to ten neutrophils were manipulated simultaneously with the proposed optical manipulation strategy (Figure S1).

Since the neutrophils were trapped at the beam focus during the optical manipulation, a dynamic rotation of the neutrophil could be expected by scanning the laser beams in a designed circular trajectory. As indicated in Figure 1e, a neutrophil was rotated around an external axis, i.e., a revolution, with a rotation radius and velocity of 2.2 μm and 10π rad/s, respectively. The revolution could be regulated by changing the scanning trajectory and frequency in real time. Furthermore, the rotation flexibility was quantified by tracking the cell center in 125 cycles, in which the rotation center could be regulated in a controlled manner (Figure 1e5). In addition, the rotation stability was characterized with the calculated rotation velocity centered at 70 μm/s (Figure 1e6). Besides, a dynamic autorotation of the neutrophil could be realized, i.e., rotation around its own axis (Figure S2).

Furthermore, the dynamic manipulation was conducted for internal granules in the neutrophil, which could be trapped stably and then rotated dynamically in a circle with a controlled diameter (Figure 1f). This subcellular manipulation shows the high spatiotemporal precision of optical manipulation. Therefore, through the programmable scanning of laser beams, the basic actions of the resting neutrophils could be fully manipulated in the living zebrafish, demonstrating great potential for further controlling their biological behaviors *in vivo*.

Optical Deformation and Activation of the Neutrophil Microcraft *In Vivo*. The circulating neutrophil in the blood vessel needs to be switched from the resting state to the activation state before fulfilling its innate biological functions.

https://doi.org/10.1021/acscentsci.2c00468
ACS Cent. Sci. 2022, 8, 1017−1027

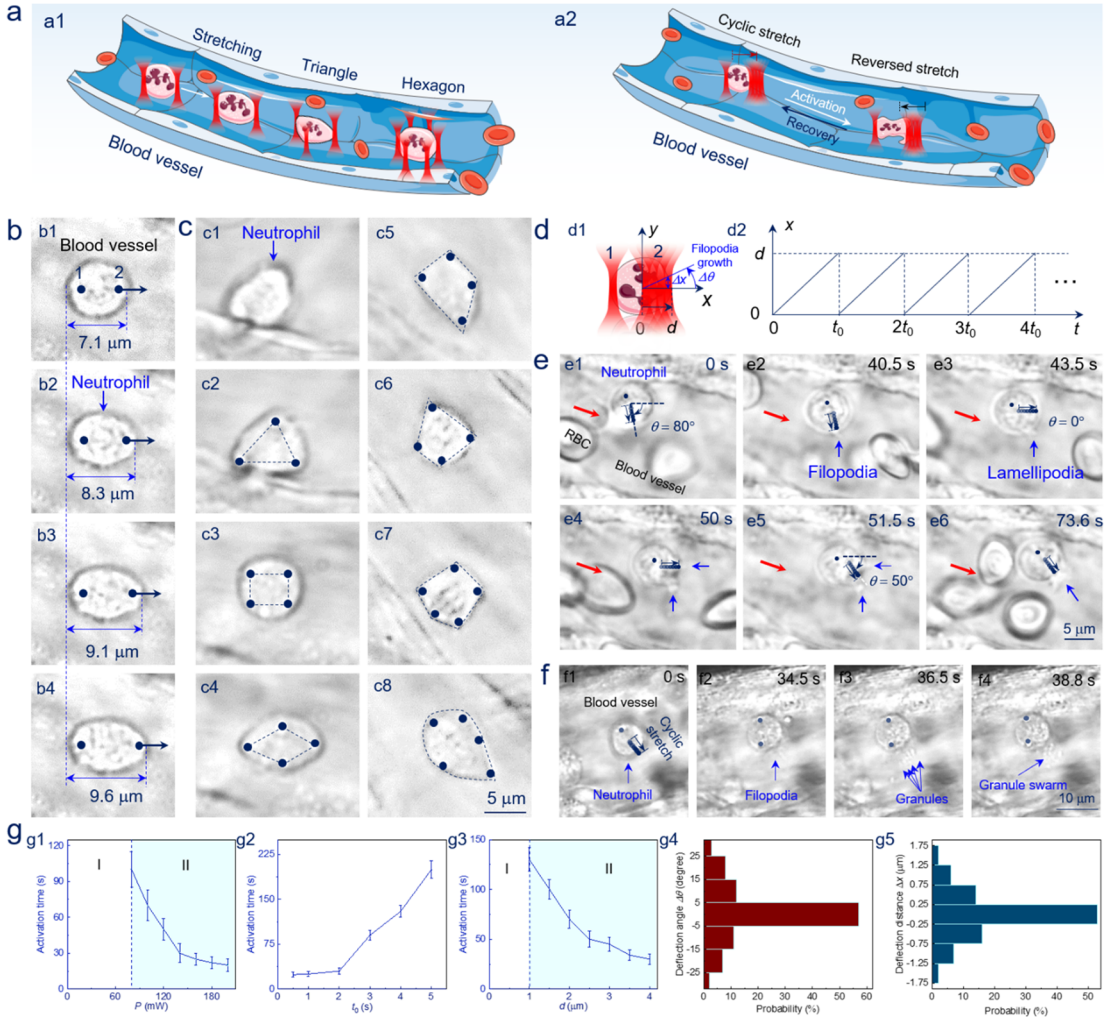

Figure 2. (a) Schematic illustration for optical deformation (a1) and activation (a2) of neutrophil *in vivo*. (b) Optical stretching of the neutrophil along the +*x* direction. (c) Optical deformation of the neutrophil into the shape of a triangle (c2), rectangle (c3), parallelogram (c4), trapezoid (c5 and c6), pentagon (c7), and water drop (c8). (d) Schematic illustration for the cyclic stretching of neutrophil (d1) with the scanning route as a function of *t* (d2). (e) Optical activation of a neutrophil with a controlled filopodia direction. (f) Optical activation of a neutrophil with induced filopodia and dynamic degranulation. (g) Calculated activation time as a function of laser power *P* (g1), scanning period t_0 (g2), and stretching length *d* (g3). All data represent means ± SD (n = 3). (g4–g5) The statistical distribution of deflection angle (g4) and distance (g5) between filopodia growth and optical stretching.

A characteristic feature of the neutrophil activation is its deformation behavior, which determines its ability in multiple processes including crawling along blood vessels, trans-endothelial migration (TEM), and tissue penetration. To explore the optically controlled deformation of neutrophils *in vivo*, multiple optical traps were applied to stretch the neutrophil by manipulating the spatiotemporal distribution of the optical force (Figure 2a1). As indicated in Figure 2b1, two optical traps were exerted on the left and right side of one neutrophil. The optical trap 1 was aimed to fix the neutrophil, while the optical trap 2 stretched it toward the right. Consequently, the trapped neutrophil started to spread along the +*x* direction, with the diameter gradually increasing from 7.1 μm to 8.3, 9.1, and 9.6 μm (Figure 2b2–b4). The neutrophil was further deformed into various shapes by multiple optical traps, e.g., a triangle shape by using three optical traps (Figure 2c2). Other shapes achieved with four or five optical traps include the rectangular, parallelogram, trapezoid, pentagon, and waterdrop shape (Figure 2c3–c8), indicating the controlled deformation ability of the optically manipulated neutrophil microcraft.

On this basis, the optically controlled neutrophil activation was further investigated. Recently, researchers have demonstrated that cyclic stretching can activate and then depolarize neutrophils *in vitro*.[37] However, it remains unknown whether mechanical stretching can activate the neutrophil *in vivo*, due to the much more complex biological surroundings of the body. Thus, cyclic stretching of the neutrophil was performed to explore the possibility of controlled activation *in vivo* (Figure 2a2), which could be determined by the real-time observation of filopodia induction and growth. A schematic illustration of the experiment design is shown in Figure 2d1. Two laser beams were designed to trap the left and right sides of a neutrophil synchronously. By the controlled programming of AOD, the right laser beam will suffer from cyclic scanning toward the +*x* direction with a scanning length of *d* and a scanning period of t_0 (Figure 2d2), under which the neutrophil might be activated in a controlled velocity and direction.

https://doi.org/10.1021/acscentsci.2c00468
ACS Cent. Sci. 2022, 8, 1017–1027

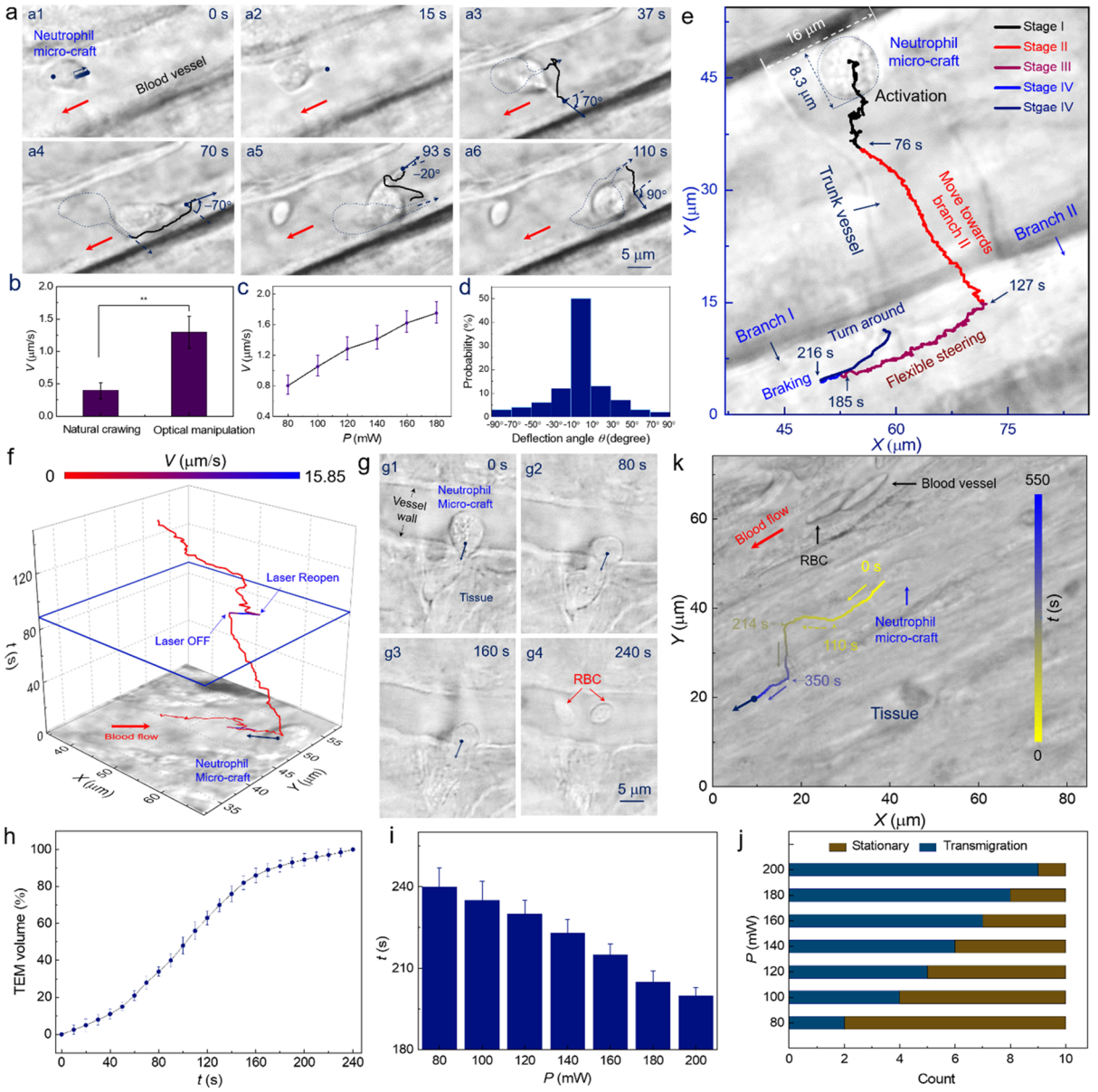

Figure 3. (a) Optical microscopic images for the targeted navigation of activated neutrophil microcraft *in vivo*. (b) The motion velocity for the neutrophil microcraft and the neutrophils in the natural crawling process. (c) The calculated velocity as a function of laser power. (d) The calculated probability as a function of the deflection angle. (e) Calculated trajectory for driving the neutrophil microcraft with flexible steering at the vessel branch. (f) The motion trajectory for navigating one neutrophil microcraft against blood flow. (g) Optical microscopic images for assisting the neutrophil microcraft to enter the vessel wall. (h) The TEM volume of neutrophil microcraft as a function of *t*. (i) The transmigration period as a function of laser power. (j) The calculated probability to assist the neutrophil microcraft transmigrate the vessel wall under various laser power. All data represent means ± SD (n = 3). (k) Optical navigation of neutrophil microcraft in deep tissue.

As shown in Figure 2e, a neutrophil was trapped by the laser beam 1 (navy dot, Figure 2e1) in the flowing blood with a velocity of 15 μm/s at t = 0 s. Meanwhile, the laser beam 2 was introduced to stretch the neutrophil with its direction toward the lower right (navy arrows, Figure 2e1). After an interval of 40.5 s, a filopodia was induced and started to grow toward the stretching direction, i.e., θ = 80° (Figure 2e2). To demonstrate the filopodia was induced by the cyclic stretching rather than a spontaneous biological process, the stretching direction was changed to be toward the right at t = 43.5 s (Figure 2e3). As a result, a second filopodia was induced and then grew along the same direction, i.e., θ = 0° (Figure 2e4). Thus, multiple filopodia could be induced while along designed directions, implying that a multifunctional activation could be achieved by manipulating the scanning route of laser beams in a programmable manner. After that, the cyclic stretching was regulated to be along the directional angle of 50° at t = 51.5 s (Figure 2e5), and consequently, two filopodia started to fuse (Figure 2e6) and then grew together along the same direction, i.e., θ = 50° (Movie S2).

Besides, the activated neutrophil could be further recovered to its original resting state by restricting its filopodia through a reversal stretching (Figure S3). Moreover, the optical force could also regulate the migration motion of naturally activated neutrophils by manipulating the existing filopodia (Figure S4).

In addition to the morphology readout, degranulation has been regarded as an indicator of neutrophil activation. As indicated in Figure 2f, one neutrophil was trapped in a blood

https://doi.org/10.1021/acscentsci.2c00468
ACS Cent. Sci. 2022, 8, 1017−1027

vessel at t = 0 s with the optical trap indicated by the navy dot. Meanwhile, a cyclic stretch was exerted on its lower right to achieve a dynamic activation (Figure 2f1). After that, the filopodia was induced along the same direction (Figure 2f2), and some granules were released from the activated neutrophil (Figure 2f3), whose amount increased continuously until the formation of a granule swarm at t = 38.8 s (Figure 2f4). The observed degranulation reconfirmed the successful neutrophil activation by optical manipulation.

Further, the activation time of the neutrophil, i.e., the time interval from initiating cyclic stretching to the filopodia formation, was characterized as a function of laser power (P), scanning period (t_0), and stretching length (d) in a quantitative manner. As shown in Figure 2g1, the neutrophil could not be activated until the laser power reached 80 mW (region I), and the activation time would decrease from 100 to 20 s with the laser power increasing from 80 to 200 mW (region II). The effect of the scanning period (t_0) on the activation time is shown in Figure 2g2. The activation time remained at 25 s when $t_0 < 2$ s and then increased with t_0 when $t_0 > 2$ s. The stretching length (d) could also regulate the activation time (Figure 2g3). When d was less than 1 μm, no sign of neutrophil activation was observed (region I). Then with the increase of d from 1 to 4 μm, the activation time was decreased from 130 to 30 s, implying that a larger stretching area will accelerate the activation process (region II). Thus, a precise activation of the neutrophil can be realized *in vivo* by regulating the detailed parameters of the scanning laser beam.

The relationship between the filopodia growth and optical stretching was further characterized in a quantified manner. As indicated in Figure 2g4 and 5, the deflection distance and angle, i.e., the interpolation of azimuthal angle and position coordinates between the filopodia growth and optical stretching, were focused in the $-15° < \theta < 15°$ and $-0.75 < \Delta x < 0.75$ μm. Thus, the filopodia mainly grew from the site of optical stretching and toward the same direction, confirming that the induction of filopodia was originated from mechanical stretching by laser rather than a random coincidence. Notably, the trapped neutrophils cannot be activated under a static optical trap without cyclic stretching (Figure S5 and Movie S3).

Targeted Migration of the Neutrophil Microcraft *In Vivo*. After activation, targeted migration of the neutrophil microcraft to the destination was expected for task execution. For this purpose, the filopodia of the activated neutrophil was manipulated by SOTs to drive the neutrophil microcraft along a designed route in a contactless and noninvasive manner. As indicated in Figure 3a1, a neutrophil was trapped in the blood vessel and activated by cyclic stretching with the laser beam on its right side, leading to a growing filopodia at t = 15 s (Figure 3a2). Then, a laser beam was applied to this filopodia to navigate the migration of the neutrophil microcraft, and the detailed motion trajectory was indicated by the black curve. When the filopodia direction was deflected with an angle of 70° at t = 37 s, the neutrophil microcraft changed its motion direction accordingly and started to migrate toward the vessel wall (the navy arrow, Figure 3a3). To demonstrate the navigation flexibility, the filopodia was further deflected with an angle of −70° at t = 70 s, and the neutrophil microcraft was thus redirected to the original direction and moved a distance of 17 μm (Figure 3a4). After that, the filopodia was deflected with an angle of −20° to drive the neutrophil microcraft toward the vessel center (Figure 3a5), followed by a deflection of 90° to transport the neutrophil microcraft toward the vessel wall again (Movie S4). Note for the optically manipulated neutrophil microcraft, their average migration velocity was 1.3 μm/s (Figure 3b), which was three times over the spontaneous crawling velocity of neutrophils (i.e., 0.3 μm/s).[31] Besides, their migration velocity increased with the laser power (Figure 3c), which reconfirmed that the optical force could accelerate the targeted migration of the neutrophil. Moreover, the calculated deflection angle θ, i.e., the azimuthal angle interpolation between the navigation of neutrophil microcraft and the exerted optical force, was focused in the range of $-10° < \theta < 10°$, indicating that the neutrophil microcraft will navigate along the same direction with the optical force (Figure 3d). Thus, under the wireless guiding of SOTs, a targeted navigation could be achieved for the neutrophil microcraft to arrive at the target sites in a designated route and controlled velocity.

The flexible steering of the neutrophil microcraft was further demonstrated at the vessel branch. As indicated in Figure 3e, a neutrophil microcraft was navigated in five stages: First, the neutrophil was activated by cyclic stretching (black curve). At t = 76 s, it started to migrate along the trunk vessel (red curve) and then encountered two branches, i.e., branch I and II. At t = 127 s, the neutrophil was intended to enter branch II. But the filopodia direction was deflected by 180° with SOT, turning the migration direction to the branch I (wine curve). At t = 185 s, the optical force was reversed toward the right. As a consequence, the neutrophil started to decelerate and finally stopped moving (blue curve). After that, the neutrophil was driven toward the right with the motion trajectory indicated by the navy curve, demonstrating a successful braking and turning around operation for the manipulated neutrophil (Figure S6 and Movie S5). These results demonstrate that the activated neutrophil microcraft can be flexibly navigated through the complex vessel network *in vivo*.

The targeted migration of the neutrophil may face multiple challenges *in vivo*, such as the blood flow and biological barriers, which need to be overcome by the optical force on the neutrophil microcraft. The actuation force of the neutrophil microcraft was first challenged by driving the activated neutrophil microcraft against the blood flow. As indicated in Figure 3f, the blood flowed in a direction toward the upper right (the red arrow) with a velocity of 15 μm/s. Meanwhile, a neutrophil was activated and then driven against the blood flow. The detailed motion trajectory was recorded as shown by the curve, in which the motion velocity was displayed by the various colors. At t = 88.8 s, the optical force was removed by turning off the laser beam. Consequently, the neutrophil changed its motion direction immediately and started to move along the blood flow (the blue curve, Figure 3f), indicating that this neutrophil could not crawl against the blood flow in a spontaneous manner. Then the optical force was reintroduced, after which the neutrophil restarted to migrate against the blood flow for a distance of 18 μm (Figure S7 and Movie S6). Furthermore, a reverse-flow migration could be achieved under a maximum flow velocity of 150 μm/s for neutrophil microcraft. Thus, the optical force applied on the neutrophil microcraft was strong enough for overcoming the blood flow *in vivo*.

The vessel wall is a major biological barrier for the neutrophils. The assisted transmigration across the vessel wall was tested for the optically manipulated neutrophil microcraft. As indicated in Figure 3g1, a neutrophil was guided

https://doi.org/10.1021/acscentsci.2c00468
ACS Cent. Sci. 2022, 8, 1017−1027

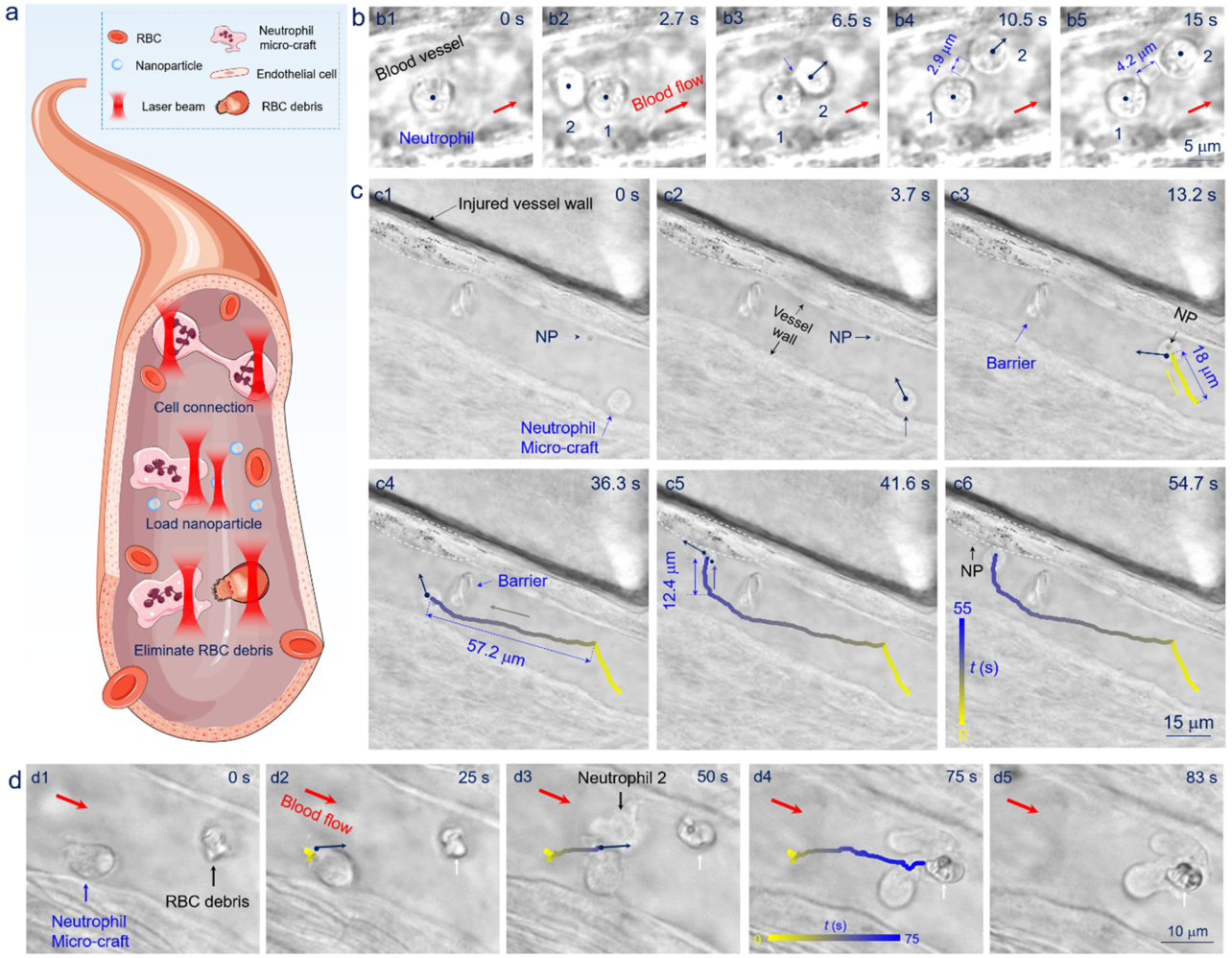

Figure 4. (a) Schematic illustration of intercellular connection, loading of nanomedicine and elimination of RBC debris with the neutrophil microcraft. (b) Optical microscopic images for the intercellular connection between two neutrophils with an adjustable protein microtube. (c) Optical microscopic images for navigating neutrophil microcraft to load nanomedicines followed by an active navigation and controlled release. (d) Optical microscopic images for navigating neutrophil microcraft to eliminate cell debris.

to approach the vessel wall by SOT. The neutrophil was originally not intended to enter the vessel wall. Nevertheless, a cyclic stretching was performed to induce the growth of filopodia toward the vessel wall. As a result, the neutrophil started to migrate across the vessel wall with its TEM volume increased with the transmigration time t (Figure 3h). At t = 240 s, the neutrophil microcraft had passed through the vessel wall and entered the tissue absolutely (Figure 3g4 and Movie S7). Besides, the neutrophil microcraft could be extracted from the vessel wall by reversing the optical force (Figure S9). Furthermore, the transmigration time exhibited a gradual decrease with the increased laser power, indicating that optical manipulation could accelerate the migration process of neutrophil microcraft (Figure 3i). Under the action of optical manipulation, not all neutrophils exhibited a desired transmigration across the vessel wall. Thus, the transmigration probability was calculated for 10 neutrophil microcraft under various powers. As indicated in Figure 3j, only two neutrophil microcraft started to transmigrate the vessel wall under the case of P = 90 mW. However, the transmigration probability was increased with the laser power and reached 9 at P = 200 mW. In addition, by integrating the targeted navigation and assisted transmigration in an organic manner, the transmigration site of the neutrophil microcraft on the vessel wall could be designated (Figure S10 and Movie S8). Therefore, the transmigration of the neutrophil microcraft across the vessel wall can be effectively controlled by SOTs, which is crucial for improving the efficiency of its task execution.

As the essential step to manipulate neutrophils toward the lesions, navigation flexibility was also explored for the transmigrated neutrophils deeper in tissue. As indicated in Figure 3k, the growth direction of filopodia was manipulated to navigate the neutrophil microcraft in a desired trajectory with controlled turning at designed site (i.e., t = 214 and 350 s). The average motion velocity was calculated to be ~0.1 μm/s (Movie S9). Therefore, it is more challenging to navigate neutrophils microcraft in tissues since the compact arrangement of tissue cells leads to a larger resistance than fluid environment in the blood vessel, and the optical force is reduced in the tissue due to a smaller refractive index contrast between the tissue cells and neutrophils.

Biomedical Applications of Optically Manipulated Neutrophil Microcraft. On the basis of the programmable manipulation of SOTs and innate functions of neutrophil, potential biomedical applications of the optically manipulated neutrophil microcraft were explored. Three possible applica-

https://doi.org/10.1021/acscentsci.2c00468
ACS Cent. Sci. 2022, 8, 1017−1027

tions are schematically shown in Figure 4a, including guided intercellular connection, nanodrug transportation, and targeted elimination of cell debris. The intercellular connection was first tested. As indicated in Figure 4b1, a neutrophil in the blood vessel (neutrophil 1) was trapped and activated at t = 0 s. At t = 2.7 s, another resting neutrophil (neutrophil 2) flowing nearby was trapped by the laser beam and contacted with neutrophil 1 (Figure 4b2). Interestingly, at t = 6.5 s, a microtube connecting the two neutrophils together was observed (Figure 4b3). Then, the position of neutrophil 2 was adjusted along the blood flow to demonstrate the microtube more clearly. Consequently, the length of the microtube was increased from 2.9 μm (Figure 4b4) to 4.2 μm (Figure 4b5), implying the existence and good elasticity of the microtube (Movie S10). Thus, it is possible to establish intercellular connection between two neutrophils through optically controlled activation and contact, which might be promising for the controlled cell communication.

Then, the loading and navigated transportation of nanomedicine was performed by hitching the neutrophil microcraft as a natural drug carrier *in vivo*. In this work, the polystyrene nanoparticle (NP) with a diameter of 500 nm was used as the model nanodrug[39−41] (Figure S11). As indicated in Figure 4c1, a neutrophil was trapped at the blood vessel, while a NP was adhered to the vessel wall at t = 0 s. However, the neutrophil did not aim to move toward the NP (Figure 4c2). At t = 3.7 s, optical manipulation was introduced to navigate the neutrophil microcraft to approach the NP to phagocytize it, like picking up a passenger (Figure 4c3).

After that, the NP-loaded neutrophil microcraft was navigated toward the injury vessel (Figure 4c4). Note that there was a biological barrier on the way, which was actively circumvented by optical navigation. Once arriving at the targeted lesion, the NP was released by trapping the neutrophil microcraft while shifting the NP out of the cell membrane (Figure 4c6), like dropping off a passenger. These results demonstrate the capability of the neutrophil microcraft in the loading and targeted transportation of nanodrugs (Movie S11). Such an NP loading and delivery process has not yet been achieved within tissues up to now, due to the larger resistance and smaller optical force in tissues.

The targeted elimination ability of the optically manipulated neutrophil microcraft was further examined. As indicated in Figure 4d1, an activated neutrophil was guided to approach the vessel wall at t = 0 s. Meanwhile, RBC debris was located at the right of neutrophil with a distance of 25 μm. However, the neutrophil microcraft remained stationary and did not crawl toward the cell debris in a spontaneous manner from 0 to 25 s (Figure 4d2). To address this issue, optical navigation was introduced at t = 25 s to drive the neutrophil microcraft in the direction of the target (Figure 4d2−5). At t = 75 s, it approached the cell debris and started to perform its phagocytosis function (Figure 4d5−6). Interestingly, another neutrophil (Neutrophil 2) emerged at t = 50 s and then tried to compete with the optically navigated neutrophil microcraft to clear the cell debris, which might be attracted by the chemokines (Movie S12). Therefore, with the active and precise control of its activation and migration *in vivo*, the neutrophil microcraft can perform its medical task at the desired time and position with enhanced efficiency.

Discussion. By combining the contactless optical tweezer and endogenous neutrophil, an optically manipulated neutrophil microcraft has been constructed, in which the scanning optical tweezer and neutrophil can be regarded as contactless remote controller and native biological material, respectively. With the real-time actuation and navigation of programmable optical manipulations, the neutrophil microcraft can be activated or recovered in a controlled manner, and the migration of the activated neutrophil microcraft is fully steerable, just like driving a vehicle. An ordinary neutrophil can also be activated as an inflammatory response and then spontaneously migrated to the targeted tissue. But its activation is largely a probabilistic event, and the subsequent migration may be slow, in the wrong direction or hindered by various obstacles.[32] With the development of optically manipulated neutrophil microcraft, the behaviors of natural neutrophil can now be actively controlled, including (1) a neutrophil microcraft can be remotely activated by SOTs at a desired time and location *in vivo*, and (2) the migration of the activated neutrophil microcraft can be precisely navigated by SOTs to achieve a designed route and velocity. On the other hand, other neutrophil-based microdevices have also been reported.[4,11,31] Among them, an excellent example is a hybrid neutrobot composed of magnetic nanoparticles and neutrophils, which was successfully navigated *in vivo* by external magnetic field to achieve targeted drug delivery toward tumor cells. Compared with the magnetic actuation strategy, our optical manipulation method has two unique advantages: (1) the ability of controlled neutrophil activation *in vivo* and (2) the precise manipulation of single neutrophil *in vivo*. Meanwhile, it also has an inherent drawback of limited tissue penetration. Recently, the manipulation depth has been pushed forward for optical tweezers with the assistance of adaptive optical microscopy[42] and optical coherence compensation technology.[43] Furthermore, by integrating fiber tweezers with optical fiber endoscopic devices, a focused laser might be introduced inside the body to manipulate neutrophils in internal tissue.

The organic combination of optical manipulation and innate functions of the neutrophil opens up new possibilities for the biomedical application of optically manipulated neutrophil microcraft. The neutrophil plays a key role in the inflammatory response and has the natural ability of phagocytosis and clearance. In this study, the optically guided intercellular connection between two neutrophils has been achieved, which might have potential to actively transfer messages between targeted neutrophils to trigger further responses.[44] For foreign agents or endogenous cell debris, the neutrophil microcraft can be immediately activated and driven toward the target to perform elimination, thus significantly enhancing the efficiency of its natural clearance ability. In addition, the neutrophil microcraft can be utilized as a drug carrier for nanomedicine. The phagocytosis ability provides efficient drug loading, while the optical manipulation ensures the targeted delivery of the nanomedicine. Compared with existing neutrophil-based drug delivery system,[45] our optically manipulated neutrophil microcraft has the advantages of endogenous material and fully active navigation for more efficient drug delivery.

Since the reported neutrophil microcraft works in living animals, attention has been paid to biological safety issues. In this work, the optical manipulation was conducted at a wavelength of 1064 nm, which has low absorption in tissue and blood cells.[46] Meanwhile, for the used maximum power of 200 mW, the heating was calculated to be 2.6 ± 0.4 °C[47] or 1.6 °C[48] in the center of optical trap, which led to no obvious cell injury during optical manipulation (Figure S12). Besides,

https://doi.org/10.1021/acscentsci.2c00468
ACS Cent. Sci. 2022, 8, 1017−1027

compared to the case *in vitro*, the laser power arrived at the intravital cell will be lower than 200 mW due to unavoidable tissue scattering. In addition, the experiments were mainly performed inside the blood vessels, and thus the heat generated by laser irradiation could not be accumulated in an efficient manner, due to the fast blood flow with a high thermal conductivity.

There are several challenging issues to be addressed for the proposed neutrophil microcraft. First, the detailed physiological mechanism remains to be explored for the cyclic-stretching-induced neutrophil microcraft activation. Considering that the growing pseudopod of the activated neutrophil microcraft originates from the actin redistribution, we suppose controlled activation of neutrophil microcraft is related to the directional shift of actin under the action of optical force. By further integrating the fluorescent labeling and lattice light sheet microscopy,[49] the distribution of actin could be observed in real time, thus offering an intuitive view to characterize the detailed activation process under cyclic stretching. Second, the number of manipulated neutrophil microcrafts needs to be further increased for more efficient target elimination in diseased tissue and the mass delivery of nanomedicines.

CONCLUSION

An optically manipulated neutrophil microcraft was constructed in living zebrafish through the integration of endogenous neutrophils and a contactless optical tweezer. By optical manipulation, the neutrophil could perform various actions *in vivo*, including directional movement, precise arrangement, controlled rotation, and deformation. In addition, the neutrophil could be remotely activated or recovered by cyclic stretching with SOTs. The activated neutrophil could be flexibly navigated to migrate in a designed route and velocity. Moreover, the optical driving force made it robust enough for crawling against blow and transmigrating across the vessel wall in a controlled manner, thus transforming the natural neutrophil into a native cellular microcraft *in vivo*. On the basis of the high-precision spatiotemporal manipulation and powerful phagocytosis ability of the neutrophil, active intercellular connection was successfully established between two neutrophil microcrafts, the loading and controlled delivery of nanomedicines was achieved by using the neutrophil microcraft as a drug carrier, and the targeted elimination of cell debris was demonstrated *in vivo*. Unlike traditional medical microdevices, this neutrophil microcraft is free from artificial microstructures and invasive implantation processes, thus avoiding complicated preparation technology and unavoidable tissue damage. Meanwhile, it exhibits high biocompatibility due to the endogenous nature and minor immunogenicity. This concept of a native neutrophil microcraft, coupled with the intelligent control of multiplexed assignment execution, could hold great promise for the active execution of complex medical tasks *in vivo*, with great potential utility in the treatment of inflammatory diseases.

METHODS

Zebrafish Care and Treatment. Adult zebrafish (90 days old, average length of 3 cm) were chosen as the model animal (Feixi Biotech. Co., Ltd., Shanghai, China). The zebrafish were maintained in a clean tank and fed with live brine shrimps. Meanwhile, the fish were cultured at 28.5 °C with a 14-h light/10-h dark cycle according to standard procedures. The used transgenic line of zebrafish was Tg(lyz:DsRed2) for visualization of the neutrophils through fluorescence labeling *in vivo*. All experiments were conducted in accordance with the ethical standards by the Laboratory Animal Ethics Committee of Jinan University.

Sample Preparation for Optical Manipulation. The zebrafish were treated with tricaine solution to achieve a general anesthesia, thus keeping the fish alive during optical manipulation, while the operated blood vessel remained stationary in the focal plane. The tricaine solution was prepared by diluting tricaine in saline with a concentration of 200 mg/L. After the preparation, each fish was placed in a Petri dish containing tricaine solution for 8 min and then moved to a cover glass (15 × 50 mm) and immobilized by 2% low melting point agarose. Meanwhile, a pipet was used to inject approximately 1 mL of tricaine solution around the zebrafish, with the aim to prevent the revival of zebrafish and maintain a stable flood flow rate of smaller than 50 μm/s in the operated vessel. Excess fluid was removed from the fish edges by using one filter paper, and then a coverslip was carefully placed on its top for a flexible manipulation. Finally, the sample was mounted on the motorized translation stage to achieve a precise position control in the $x-y$ plane.

Experiment Setup. The experiment setup was constructed around a scanning optical tweezers system (Tweez250si, Aresis Co., Ltd., Slovenia) for a flexible optical manipulation. To achieve a high penetration depth, the wavelength at 1064 nm was chosen for the trapping laser, which exhibits a weak tissue absorption and induces limited optothermal damage. The incident laser beam will interact with the integrated acousto-optic deflector (AOD), after which the laser could be deflected at a tunable angle and distance. The AOD has a maximum switching rate of 100 kHz, and thus the spatial-temporal distribution of laser beams could be regulated in real time. The laser beam was expanded through a beam expander to overfill the pupil of microscope objective and then reflected upward by the dichroic mirror. Finally, the laser was refocused into the tail of an adult zebrafish after passing through the pupil of a 60× water immersion microscope objective (CFI Apo, NA = 1.0). The illumination light was focused through a condenser for irradiating the sample. The experimental process was recorded by a high-speed complementary metal-oxide-semiconductor camera (IDS Imaging Development Systems GmbH, Germany, 20 frames per second) and then displayed on the computer screen for real-time image acquisition and video recording.

Injection of PS Nanoparticles into the Zebrafish. The PS nanoparticles were commercially available (Huge Biotech. Co., Ltd., Shanghai, China) with an average diameter of 500 nm. The concentration used for injection was ∼5 × 10^6 nanoparticles/mL, which was prepared by diluting the nanoparticles with phosphate buffer solution. The sample was ultrasonicated for 10 min to achieve a monodisperse nanoparticle solution. After that, the sample was loaded into a glass micropipette (Gaierdena Co., Ltd., Wuhan, China) with the outer and inner diameter of 1.14 and 0.5 mm, respectively. To ensure a precise injection with less physiological damage, the micropipette was stretched by a micropipette puller, and the diameter of micropipette tip was decreased to be 5−10 μm. Finally, the fabricated micropipette was placed on a programmable nanoliter injector (Nanojet III, Drummond Co., Ltd., USA), and 10 nL nanoparticle solution was injected into the posterior cardinal vein of the zebrafish. The injection process was monitored on the computer screen in real time.

https://doi.org/10.1021/acscentsci.2c00468
ACS Cent. Sci. 2022, 8, 1017−1027

Preparation of RBC Debris. The RBC debris was created by the dynamic stretching technique with the assistance of dual laser beams. In detail, two optical traps were designed to trap the left and right side of RBC simultaneously. After that, the right optical trap was shifted toward the right gradually, while the left optical trap remained stationary. Meanwhile, the RBC was stretched toward the right and finally broken into cell debris.

Data Analysis. The cell/morphological outlines were determined through the quantitative recognition for the gray values of acquired images by using the ImageJ software, while for the detailed motion trajectory, a high-speed CCD camera was used to record the experiment progress in real time with a maximum frame rate of 60 Hz. After that, the location coordinates were calculated for the targeted neutrophil cell from the video analysis with the assistance of manual tracking plugin in ImageJ software. Furthermore, the detailed motion trajectory was drawn through the Origin software.

■ ASSOCIATED CONTENT

Supporting Information

The Supporting Information is available free of charge at https://pubs.acs.org/doi/10.1021/acscentsci.2c00468.

Simultaneous manipulation of multiple neutrophils, dynamic revolution and rotation of neutrophil, optical activation of neutrophils, flexible steering and optical navigation of neutrophil microcraft, assisted transmigration of neutrophil microcraft, SEM image and size distribution of PS nanoparticles, viability characterization of optically manipulated neutrophils and supplementary discussion (PDF)

Motion control of neutrophils in vivo (MP4)

Optical deformation and activation of neutrophils in a desired direction (MP4)

Simultaneous manipulation of multiple neutrophils with selective activation (MP4)

Targeted navigation of neutrophil microcraft *in vivo* (MP4)

Flexible steering of neutrophil microcraft *in vivo* (MP4)

Optical navigation of neutrophil microcraft against blood flow *in vivo* (MP4)

Assisted transmigration of neutrophil microcraft across the vessel wall (MP4)

Assisted transmigration of neutrophil microcraft at targeted site *in vivo* (MP4)

Targeted navigation of neutrophil microcraft in tissue (MP4)

Optically controlled intercellular connection between two neutrophils *in vivo* (MP4)

Targeted delivery of nanoparticles with neutrophil microcraft *in vivo* (MP4)

Targeted elimination of cell debris with neutrophil microcraft *in vivo* (MP4)

■ AUTHOR INFORMATION

Corresponding Authors

Xianchuang Zheng − *Institute of Nanophotonics, Jinan University, Guangzhou 511443, China;* orcid.org/0000-0002-1076-8959; Email: xczheng@jnu.edu.cn

Baojun Li − *Institute of Nanophotonics, Jinan University, Guangzhou 511443, China*; Email: baojunli@jnu.edu.cn

Authors

Xiaoshuai Liu − *Institute of Nanophotonics, Jinan University, Guangzhou 511443, China;* orcid.org/0000-0001-5665-7421

Qing Gao − *Institute of Nanophotonics, Jinan University, Guangzhou 511443, China*

Shuai Wu − *Institute of Nanophotonics, Jinan University, Guangzhou 511443, China*

Haifeng Qin − *Institute of Nanophotonics, Jinan University, Guangzhou 511443, China*

Tiange Zhang − *Institute of Nanophotonics, Jinan University, Guangzhou 511443, China*

Complete contact information is available at: https://pubs.acs.org/10.1021/acscentsci.2c00468

Author Contributions

#X.L. and Q.G. contributed equally to this work.

Notes

The authors declare no competing financial interest.

■ ACKNOWLEDGMENTS

This work was supported by the National Natural Science Foundation of China (Nos. 22175078 and 11904134), the Basic and Applied Basic Research Foundation of Guangdong Province (No. 2020A1515110653), and the Science and Technology Program of Guangzhou (No. 201904010411).

■ REFERENCES

(1) Soto, F.; Wang, J.; Ahmed, R.; Demirci, U. Medical micro/nanorobots in precision medicine. *Adv. Sci.* **2020**, *7*, 2002203.

(2) Wu, Z.; Chen, Y.; Mukasa, D.; Pak, O. S.; Gao, W. Medical micro/nanorobots in complex media. *Chem. Soc. Rev.* **2020**, *49*, 8088−8112.

(3) Aziz, A.; Pane, S.; Iacovacci, V.; Koukourakis, N.; Czarske, J.; Menciassi, A.; Medina-Sánchez, M.; Schmidt, O. G. Medical imaging of microrobots: Toward in vivo applications. *ACS Nano* **2020**, *14*, 10865−10893.

(4) Wang, B.; Kostarelos, K.; Nelson, B. J.; Zhang, L. Trends in micro-/nanorobotics: Materials development, actuation, localization, and system integration for biomedical applications. *Adv. Mater.* **2021**, *33*, 2002047.

(5) Soto, F.; Karshalev, E.; Zhang, F.; Esteban Fernandez de Avila, B.; Nourhani, A.; Wang, J. Smart materials for microrobots. *Chem. Rev.* **2022**, *122*, 5365−5403.

(6) Dai, B.; Wang, J.; Xiong, Z.; Zhan, X.; Dai, W.; Li, C.-C.; Feng, S.-P.; Tang, J. Programmable artificial phototactic microswimmer. *Nat. Nanotechnol* **2016**, *11*, 1087−1092.

(7) Schwarz, L.; Karnaushenko, D. D.; Hebenstreit, F.; Naumann, R.; Schmidt, O. G.; Medina-Sánchez, M. A rotating spiral micromotor for noninvasive zygote transfer. *Adv. Sci.* **2020**, *7*, 2000843.

(8) Sitti, M.; Wiersma, D. S. Pros and cons: Magnetic versus optical microrobots. *Adv. Mater.* **2020**, *32*, 1906766.

(9) Xu, H.; Medina-Sánchez, M.; Maitz, M. F.; Werner, C.; Schmidt, O. G. Sperm micromotors for cargo delivery through flowing blood. *ACS Nano* **2020**, *14*, 2982−2993.

(10) Bozuyuk, U.; Yasa, O.; Yasa, I. C.; Ceylan, H.; Kizilel, S.; Sitti, M. Light-triggered drug release from 3D-printed magnetic chitosan microswimmers. *ACS Nano* **2018**, *12*, 9617−9625.

(11) Schmidt, C. K.; Medina-Sánchez, M.; Edmondson, R. J.; Schmidt, O. G. Engineering microrobots for targeted cancer therapies from a medical perspective. *Nat. Commun.* **2020**, *11*, 1−18.

(12) Nelson, B. J.; Kaliakatsos, I. K.; Abbott, J. J. Microrobots for minimally invasive medicine. *Annu. Rev. Biomed. Eng.* **2010**, *12*, 55−85.

(13) Li, J.; Esteban-Fernandez de Avila, B.; Gao, W.; Zhang, L.; Wang, J. Micro/nanorobots for biomedicine: Delivery, surgery, sensing, and detoxification. *Sci. Robot.* **2017**, *2*, No. eaam6431.
(14) Chu, D.; Dong, X.; Shi, X.; Zhang, C.; Wang, Z. Neutrophil-based drug delivery systems. *Adv. Mater.* **2018**, *30*, 1706245.
(15) Joh, H.; Fan, D. E. Materials and schemes of multimodal reconfigurable micro/nanomachines and robots: Review and perspective. *Adv. Mater.* **2021**, *33*, 2101965.
(16) Chu, D.; Gao, J.; Wang, Z. Neutrophil-mediated delivery of therapeutic nanoparticles across blood vessel barrier for treatment of inflammation and infection. *ACS Nano* **2015**, *9*, 11800−11811.
(17) Timin, A. S.; Litvak, M. M.; Gorin, D. A.; Atochina-Vasserman, E. N.; Atochin, D. N.; Sukhorukov, G. B. Cell-based drug delivery and use of nano-and microcarriers for cell functionalization. *Adv. Healthc. Mater.* **2018**, *7*, 1700818.
(18) Thanuja, M. Y.; Anupama, C.; Ranganath, S. H. Bioengineered cellular and cell membrane-derived vehicles for actively targeted drug delivery: So near and yet so far. *Adv. Drug Delivery Rev.* **2018**, *132*, 57−80.
(19) Villa, C. H.; Anselmo, A. C.; Mitragotri, S.; Muzykantov, V. Red blood cells: Supercarriers for drugs, biologicals, and nanoparticles and inspiration for advanced delivery systems. *Adv. Drug Deliver. Rev.* **2016**, *106*, 88−103.
(20) Li, Y.; Liu, X.; Xu, X.; Xin, H.; Zhang, Y.; Li, B. Red-blood-cell waveguide as a living biosensor and micromotor. *Adv. Funct. Mater.* **2019**, *29*, 1905568.
(21) Wu, Z.; Li, T.; Li, J.; Gao, W.; Xu, T.; Christianson, C.; Gao, W.; Galarnyk, M.; He, Q.; Zhang, L.; Wang, J. Turning erythrocytes into functional micromotors. *ACS Nano* **2014**, *8*, 12041−12048.
(22) Esteban-Fernández de Ávila, B.; Gao, W.; Karshalev, E.; Zhang, L.; Wang, J. Cell-like micromotors. *Acc. Chem, Res.* **2018**, *51*, 1901−1910.
(23) Ley, K.; Hoffman, H. M.; Kubes, P.; Cassatella, M. A.; Zychlinsky, A.; Hedrick, C. C.; Catz, S. D. Neutrophils: New insights and open questions. *Sci. Immunol.* **2018**, *3*, No. eaat4579.
(24) Borregaard, N. Neutrophils, from marrow to microbes. *Immunity* **2010**, *33*, 657−670.
(25) De Oliveira, S.; Rosowski, E. E.; Huttenlocher, A. Neutrophil migration in infection and wound repair: going forward in reverse. *Nat. Rev. Immunol* **2016**, *16*, 378−391.
(26) Richards, D. M.; Endres, R. G. How cells engulf: a review of theoretical approaches to phagocytosis. *Rep. Prog. Phys.* **2017**, *80*, 126601.
(27) Keshavan, S.; Calligari, P.; Stella, L.; Fusco, L.; Delogu, L. G.; Fadeel, B. Nano-bio interactions: a neutrophil-centric view. *Cell Death Dis.* **2019**, *10*, 1−11.
(28) Xue, J.; Zhao, Z.; Zhang, L.; Xue, L.; Shen, S.; Wen, Y.; Wei, Z.; Wang, L.; Kong, L.; Sun, H.; Ping, Q.; Mo, R.; Zhang, C. Neutrophil-mediated anticancer drug delivery for suppression of postoperative malignant glioma recurrence. *Nat. Nanotechnol.* **2017**, *12*, 692−700.
(29) Chu, D.; Dong, X.; Zhao, Q.; Gu, J.; Wang, Z. Photosensitization priming of tumor microenvironments improves delivery of nanotherapeutics via neutrophil infiltration. *Adv. Mater.* **2017**, *29*, 1701021.
(30) Wang, Z.; Li, J.; Cho, J.; Malik, A. B. Prevention of vascular inflammation by nanoparticle targeting of adherent neutrophils. *Nat. Nanotechnol* **2014**, *9*, 204−210.
(31) Zhang, H.; Li, Z.; Gao, C.; Fan, X.; Pang, Y.; Li, T.; Wu, Z.; Xie, H.; He, Q. Dual-responsive biohybrid neutrobots for active target delivery. *Sci. Robot.* **2021**, *6*, No. 9519eaaz.
(32) Han, Y.; Zhao, R.; Xu, F. Neutrophil-Based Delivery Systems for Nanotherapeutics. *Small* **2018**, *14*, 1801674.
(33) Pires, R. H.; Felix, S. B.; Delcea, M. The architecture of neutrophil extracellular traps investigated by atomic force microscopy. *Nanoscale* **2016**, *8*, 14193−14202.
(34) Hamza, B.; Irimia, D. Whole blood human neutrophil trafficking in a microfluidic model of infection and inflammation. *Lab Chip* **2015**, *15*, 2625−2633.
(35) Ekpenyong, A. E.; Toepfner, N.; Fiddler, C.; Herbig, M.; Li, W.; Cojoc, G.; Summers, C.; Guck, J.; Chilvers, E. R. Mechanical deformation induces depolarization of neutrophils. *Sci. Adv.* **2017**, *3*, No. e1602536.
(36) Gao, Q.; Wang, W.; Li, X.; Li, Y.; Ferraro, P.; Jiao, X.; Liu, X.; Zhang, Y.; Li, B. Cell nucleus as an endogenous biological micropump. *Biosens. Bioelectron* **2021**, *182*, 113166.
(37) Dholakia, K.; Drinkwater, B. W.; Ritsch-Marte, M. Comparing acoustic and optical forces for biomedical research. *Nat. Rev. Phys.* **2020**, *2*, 480−491.
(38) Robertson, A. L.; Holmes, G. R.; Bojarczuk, A. N.; Burgon, J.; Loynes, C. A.; Chimen, M.; Sawtell, A. K.; Hamza, B.; Willson, J.; Walmsley, S. R.; Anderson, S. R.; Coles, M. C.; Farrow, S. N.; Solari, R.; Jones, S.; Prince, L. R.; Irimia, D.; Rainger, G. E.; Kadirkamanathan, V.; Whyte, M. K. B.; Renshaw, S. A. A zebrafish compound screen reveals modulation of neutrophil reverse migration as an anti-inflammatory mechanism. *Sci. Transl. Med.* **2014**, *6*, 225ra29.
(39) Beckers, S. J.; Staal, A. H.; Rosenauer, C.; Srinivas, M.; Landfester, K.; Wurm, F. R. Targeted drug delivery for sustainable crop protection: transport and stability of polymeric nanocarriers in plants. *Adv. Sci.* **2021**, *8*, 2100067.
(40) Li, L.; Sun, S.; Tan, L.; Wang, Y.; Wang, L.; Zhang, Z.; Zhang, L. Polystyrene nanoparticles reduced ROS and inhibited ferroptosis by triggering lysosome stress and TFEB nucleus translocation in a size-dependent manner. *Nano Lett.* **2019**, *19*, 7781−7792.
(41) Dos Santos, T.; Varela, J.; Lynch, I.; Salvati, A.; Dawson, K. A. Quantitative assessment of the comparative nanoparticle-uptake efficiency of a range of cell lines. *Small* **2011**, *7*, 3341−3349.
(42) Yoon, S.; Kim, M.; Jang, M.; Choi, Y.; Choi, W.; Kang, S.; Choi, W. Deep optical imaging within complex scattering media. *Nat. Rev. Phys.* **2020**, *2*, 141−158.
(43) Xu, X.; Liu, H.; Wang, L. V. Time-reversed ultrasonically encoded optical focusing into scattering media. *Nat. Photon* **2011**, *5*, 154−157.
(44) Nahrendorf, M.; Swirski, F. K. Neutrophil-macrophage communication in inflammation and atherosclerosis. *Science* **2015**, *349*, 237−238.
(45) Vishnevskiy, D. A.; Garanina, A. S.; Chernysheva, A. A.; Chekhonin, V. P.; Naumenko, V. A. Neutrophil and nanoparticles delivery to tumor: Is it going to carry that weight? *Adv. Healthc. Mater.* **2021**, *10*, 2002071.
(46) Zhong, M.; Wei, X.; Zhou, J.; Wang, Z.; Li, Y. Trapping red blood cells in living animals using optical tweezers. *Nat. Commun.* **2013**, *4*, 1−7.
(47) Ebert, S.; Travis, K.; Lincoln, B.; Guck, J. Fluorescence ratio thermometry in a microfluidic dual-beam laser trap. *Opt. Express* **2007**, *15*, 15493−15499.
(48) Peterman, E. J.; Gittes, F.; Schmidt, C. F. Laser-induced heating in optical traps. *Biophys. J.* **2003**, *84*, 1308−1316.
(49) Fritz-Laylin, L. K; Riel-Mehan, M.; Chen, B.-C.; Lord, S. J; Goddard, T. D; Ferrin, T. E; Nicholson-Dykstra, S. M; Higgs, H.; Johnson, G. T; Betzig, E.; Mullins, R D. Actin-based protrusions of migrating neutrophils are intrinsically lamellar and facilitate direction changes. *Elife* **2017**, *6*, No. e26990.

https://doi.org/10.1021/acscentsci.2c00468
ACS Cent. Sci. 2022, 8, 1017−1027